Assessment of the Intestinal Absorption of Higher Olefins by the Everted Gut Sac Model in Combination with In Silico New Approach Methodologies

Quan Shi,* Juan-Carlos Carrillo, Michael G. Penman, Jason Manton,* Elena Fioravanzo, Robert H. Powrie, Clifford R. Elcombe, Tilly Borsboom-Patel, Yuan Tian, Hua Shen, and Peter J. Boogaard

Read Online

ACCESS | Metrics & More | Article Recommendations | Supporting Information

ABSTRACT: To reduce the number of animals and studies needed to fulfill the information requirements as required by Registration, Evaluation, Authorisation and Restriction of Chemicals (REACH) (EC no. 1907/2006), a read-across approach was used to support approximately 30 higher olefins. This study aimed to assess the absorption potential of higher olefins through the gut wall as the experimentally determined bioavailability which would strengthen the read-across hypothesis and justification, reducing the need for toxicity studies on all of the higher olefins. The absorption potential of a series of higher olefins (carbon range from 6 to 28, with five configurations of the double bond) was determined in the in vitro everted rat small intestinal sac model

Everted rat small intestine

and subsequently ranked. In addition, in silico approaches were applied to predict the reactivity, lipophilicity, and permeability of higher olefins. In the in vitro model, everted sacs were incubated in "fed-state simulated small intestinal fluid" saturated with individual higher olefins. The sac contents were then collected, extracted, and analyzed for olefin content using gas chromatography with a flame ionization detector. The C6 to C10 molecules were readily absorbed into the intestinal sacs. Marked inter-compound differences were observed, with the amount of absorption generally decreasing with the increase in carbon number. Higher olefins with ≥C14 carbons were either not absorbed or very poorly absorbed. In the reactivity simulation study, the reactivity is well described by the position of the double bond rather than the number of carbon atoms. In the lipophilicity and permeability analysis, both parameter descriptors depend mainly on the number of carbon atoms and less on the position of the double bond. In conclusion, these new approach methodologies provide supporting information on any trends or breakpoints in intestinal uptake and a hazard matrix based on carbon number and position of the double bond. This matrix will further assist in the selection of substances for inclusion in the mammalian toxicity testing programme.
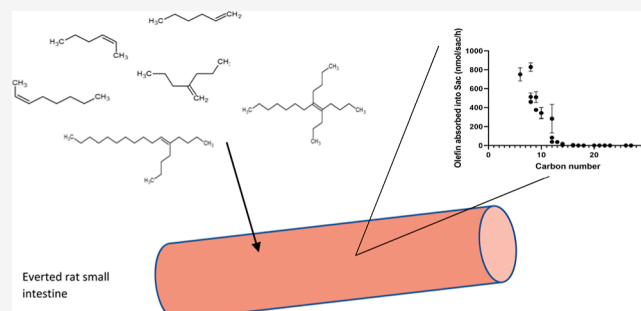
1. INTRODUCTION

Higher olefins, which have the general formula C_nH_{2n}, belong to the family of unsaturated hydrocarbons, and are structurally similar to paraffins but contain two fewer hydrogen atoms providing a single double bond between adjacent carbon atoms.[1] Higher olefins are widely used as key raw materials for producing a wide range of products, from detergents, cleaning products, and sun creams to plastics, lubricants, and drilling fluids.[2] Higher olefins can be produced from refinery streams or synthesized via ethylene and/or propylene oligomerization with carbon chain lengths ranging from C6 to C54.[3] Refinery olefins are highly branched, while synthetic olefins are mostly linear. In general, based on the position of the double bond, there are four types of higher olefins (Figure 1):

1. Linear α olefins (i.e., vinyl—straight chain with a single double bond in the α position),

2. linear internal olefins (i.e., cis/trans disubstituted—straight chain with a single double bond in an internal position),

3. branched α olefins (i.e., vinylidene—isomerized olefins with a single double bond in the α position), and

4. branched internal olefins (i.e., trisubstituted and tetrasubstituted—isomerized olefins with a single double bond in an internal position).
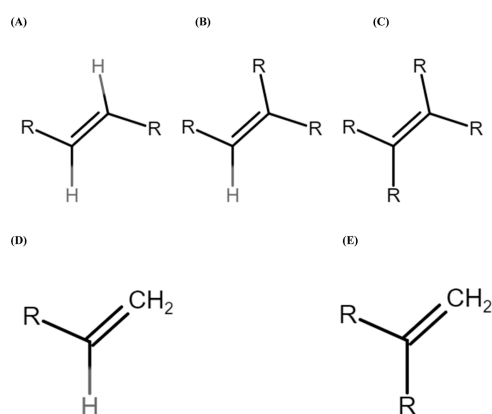
Figure 1. Various olefins and branching units referred to in the following as follows: (A) cis/trans disubstituted (linear internal); (B) trisubstituted (branched internal); (C) tetrasubstituted (branched internal); (D) vinyl (linear α); and (E) vinylidene (branched α).

Limited published data are available for the safety assessment of higher olefins. In addition, the safety profile of higher olefins has been hampered by the lack of assessment of intestinal absorption of potentially bioactive compounds. Hence, information regarding the bioavailability of higher olefins would be crucial to support read across among the higher olefins to meet the information requirements of Registration, Evaluation, Authorisation and Restriction of Chemicals (REACH) EC no. 1907/2006.[4] Any substance administered must be able to reach its site of action to exert an effect on a living organism.[5] Because oral exposure is the preferred administration route by the regulatory authorities, gastrointestinal (GI) bioavailability is an important factor in hazard assessment. Hence, it is critical to investigate the absorption potential of higher olefins through the gut wall to help determine their toxicity profile. The bioavailability of a substance is affected by various factors, such as solubility, partition coefficient, particle size, and presence of salts or isomers; in most cases, the major determining factors are likely to be metabolism (i.e., reactivity) and absorption (i.e., permeability) at the intestinal level.[6] Moreover, lipophilicity shall also be considered as it is strongly

Table 1. Higher Olefins Chemical Information

HOPA code	name	CAS no.	substances type	carbon number	molecular weight (g/mol)	density at 20 °C[a]
1	1-hexene	592-41-6	mono-constituent	6	84	0.673
2	1-octene	111-66-0	mono-constituent	8	112	0.715
3	1-decene	872-05-9	mono-constituent	10	140	0.74
4	1-tetradecene-MC	1120-36-1	mono-constituent	14	196	0.771
5	1-tetradecene-UVCB	1120-36-1	UVCB	14	196	0.771
6	1-dodecene	112-41-4	mono-constituent	12	168	0.758
7	1-hexadecene-MC	629-73-2	mono-constituent	16	224	0.78
8	1-hexadecene-UVCB	629-73-2	mono-constituent	16	224	0.78
9	1-octadecene-MC	112-88-9	mono-constituent	18	252	0.793
10	1-octadecene-UVCB	112-88-9	UVCB	18	252	0.793
11[b]	alkenes, C20−24 α-	93924-10-8	UVCB	22	308	0.815 (17)
12	alkenes, C20−24 α-	93924-10-8	UVCB	22	308	0.79
13[b]	alkenes, C26−28 α-	no data supplied	multi-constituent	27	378	0.8
14[b]	alkenes, C20 + α-	no data supplied	no data supplied	20	280	
15	octene	no data supplied	no data supplied	8	112	0.715
16	decene	25339-53-1	UVCB	10	140	0.74
17	hexadecene	26952-14-7	UVCB	16	224	0.78 (?)
18	nonene	27215-95-8	mono-constituent	9	126	
19	octadecene	27070-58-2		18	252	0.79
20	alkenes, C10−14	85681-75-0	UVCB	12		
21	alkenes C11/C13/C14 (aka tridecene) (aka alkenes C13−14)	25377-82-6	UVCB	13		
22	alkenes C10/C11/C12/C13 (aka alkenes C11−12)	no data supplied	UVCB	12		
23	alkenes, C8−10, C9-rich	68526-55-6	UVCB	9	126	0.739 (16)
24	alkenes, C15−18	93762-80-2	UVCB	16		
25	alkenes, C16−18	(formerly 148617-57-6 and 148617-59-8)	UVCB	17		
26	alkenes, C19−23 (aka hydrocarbons, C12−30, olefin-rich, ethylene polymn. by-product)	no CAS	UVCB	21	294	0.802 (21)
27	alkenes, C20−24 (aka C20−C22 (even numbered, linear and branched) and C24 (branched) alkenes)	no CAS	no data supplied	23		
28[b]	alkenes, C24−28 (aka alkenes, C21−32 linear and branched)	no CAS	UVCB	26	378	0.823 (40)
29	hexadecene	no data supplied	UVCB	16	224	
30	iso-octene	no data supplied	no data supplied	8	112	

[a]Number in parenthesis is temperature if not 20 °C. [b]Compounds were insoluble in the FeSSIF media; MC: mono-constituent; UVCB: unknown or variable composition, complex reaction products or of biological materials.

correlated with the intestinal permeability, which are the two factors affecting oral bioavailability.[7]

The mechanism of the intestinal absorption of chemical compounds has been studied for several decades via different in vivo and in vitro techniques such as the Ussing chamber, isolated epithelial cells, and the everted gut sac model. The everted sac model was first introduced in 1954 by Wilson and Wiseman[8] to study intestinal drug transport. Because then the model has been improved and is applied to pharmaceutical and chemical field for several purposes: kinetic mechanism, absorption, metabolism, transport, and so forth. Although several species are suitable to apply this technique, the rat is the most used species for in vitro studies. Indeed, as a model for human investigation, the rat offers many advantages over the other species and the rat has become a standardized physiological and toxicological model for pharmaceutical and other industrial research.[9] Anatomy-wise, the digestive systems of humans and rats are much in common regarding the structure and functions of the organs, the significance of which is in the perception, mechanical and chemical (enzymatic) digestion, and absorption of the nutrients into the body.[10]

Therefore, in this study, the in vitro everted rat small intestinal sac method is used to determine and rank the intestinal absorption potential of a series of higher olefins with different types of double bonds (i.e., linear α, linear internal, branched α, branched internal—trisubstituted, and branched internal—tetrasubstituted) as well as carbon number (range from C6 to C28). At the same time, an in silico approach was applied to predict the reactivity, lipophilicity, and permeability of the same higher olefins to compare with the in vitro absorption data. The additional data not only provide information on any trends or breakpoints of higher olefins in intestinal uptake but also may assist in explaining the toxicity observed in the chemical safety assessment.

2. MATERIALS AND METHODS

2.1. Test Item and Reagents. All the higher olefins examined were supplied by higher olefins and poly αolefins (HOPA) consortium and are shown in Table 1. Iso-octane SupraSolv and n-hexane for gas chromatography were obtained from Merck, UK. Simulated intestinal fluid (SIF) powder was obtained from Biorelevant, Switzerland. TC-199 tissue culture media was obtained from Sigma-Aldrich, UK.

2.2. Preparation of "Fed State"-SIF. An acetate buffer was prepared by dissolving NaOH (4.04 g), glacial acetic acid (8.65 g), and NaCl (11.87 g) in 0.9 L of purified water. The pH was adjusted to 5.0 using NaOH (1 M) and the volume made up to 1 L with purified water.

"Fed State"-SIF (FeSSIF) was prepared by adding SIF Powder (11.2 g) to approximately 500 mL of acetate buffer, with stirring until dissolved, and then making up to volume (1 L) with the buffer.

2.3. Eversion of Rat Proximal Small Intestine and Incubations with Test Items. Male Han Wistar rats (approx. 8−12 weeks old) were obtained from Harlan, Bicester, UK. The study was designed and conducted to cause the minimum suffering or distress to the animals consistent with the scientific objectives and in accordance with the CXR Biosciences Ltd., Dundee, United Kingdom policy on animal welfare and the requirements of the United Kingdom's Animals (Scientific Procedure) Act 1986. The conduct of the study may be reviewed, as part of the CXR Biosciences, Dundee, United Kingdom Ethical Review Process.

The everted intestinal sacs were prepared by gently everting a freshly excised rat proximal small intestine over a glass stirring rod, rinsing with TC-199 media and filling the everted intestine with oxygenated FeSSIF medium at 37 °C and dividing it into sacs approximately 2.5 cm in length using braided suture silk.

Each sac was placed in a flask containing 10 mL of FeSSIF medium at 37 °C with added individual α-olefins (20 μL). The incubations were

performed in triplicate at 37 °C for 1 h. After 1 h, the individual sacs were removed, washed with running water, and blotted dry. The sacs were cut open and the serosal fluid drained into small tubes. Each tube was weighed before and after the collection of the serosal fluid to accurately calculate the volume of medium collected from inside the sac.

2.4. Extraction of Higher Olefins from FeSSIF Media. A sample of each FeSSIF medium containing individual higher olefins was taken before the addition of the everted intestinal sacs and serially diluted (1:10) four times to prepare a series of calibration standards. 400 μL of each calibration standard was extracted as below. These were given the nominal concentration values of 2000, 200, 20, 2, and 0.2 μg/mL and subsequently corrected for the results using the individual densities of each individual higher olefin in Table 1.

The contents of each sac (400 μL) and a sample of the external medium after incubation (400 μL) were extracted using 1 mL of either n-hexane (for 1-octene, octene, nonene, and iso-octene) or iso-octane solvent (for all other higher olefins). This mixture was gently vortexed for approximately 5 min and then centrifuged at 4,000g for 15 min.

A 200 μL sample of the supernatant was removed and placed in a crimp-top vial for analysis by gas chromatography with flame ionization detection (GC-FID) to determine the concentration of higher olefin in each sample.

2.5. Gas Chromatography Flame Ionization Detection. The GC-FID system consisted of a Varian 3800 gas chromatograph fitted with flame ionization detector using a fused silica capillary column (10 m length × 0.1 mm internal diameter) and hydrogen as the carrier gas. The column temperature was programmed to start at 40 °C and then raised at 20 °C/min to 250 °C with a total run time of 12.5 min. The injector volume was 1 μL and injector temperature was 270 °C. The data were processed with Varian Galaxie Chromatography Workstation version 1.8.501.1. The calibration curves were linear from 0.2 μg/mL to 2 mg/mL for each of the higher olefins. Appropriate dilutions were carried out to obtain concentrations in the range of the calibration conditions where needed. The system showed no interference from other components in the samples.

2.6. Computational Simulation. *2.6.1. Prediction of Reactivity.* The reactivity of the olefins was characterized by means of quantum mechanics (QM), and ChemTunes·ToxGPS v3 (MN-AM https://www.mn-am.com/) and CORINA Symphony v1.1 (MN-AM https://www.mn-am.com/) were used to calculate the molecular and the QM descriptors.

The series of compounds is characterized by a variable number of carbon atoms from 6 to 28 and five combinations of position and substitution of the double bond described below:

1. linear α
2. linear internal (disubstituted)
3. branched α (vinylidene)
4. branched internal—trisubstituted
5. branched internal—tetrasubstituted

In the following analysis, the isomers are named with a code such as C6-a-1 where: C6 defines the number of carbon atoms of the isomer, the letter -a- defines the position and substitution of the double bond (-a- for α double bond, -di- for internal di substituted double bond, -vi- for vinylidene (R2C=CH2), -tri- for tri substituted double bond, and -tetra- for tetra substituted double bond). The number after the letter defines the order of the isomers generated from the simulation.

The SMILES of the isomers (i.e., C6, C8, and C20) used in this analysis are showed in Tables S1 and S2 in the Supporting Information.

In addition, to cover the whole series of higher olefins, a total 115 isomers with the number of carbon atoms ranging from C6 to C28 and five configurations of the double bond (α, di-substituted, tri-substituted, tetra-substituted, and vinyl) for each chain length were included in the following analysis (Table S3 in the Supporting Information).

2.6.2. Prediction of Lipophilicity and Permeability. Lipophilicity is a parameter of a chemical substance which can provide information of its permeability to reach the target tissue in the body.[11] The log P coefficient is well-known as one of the principal parameters for the
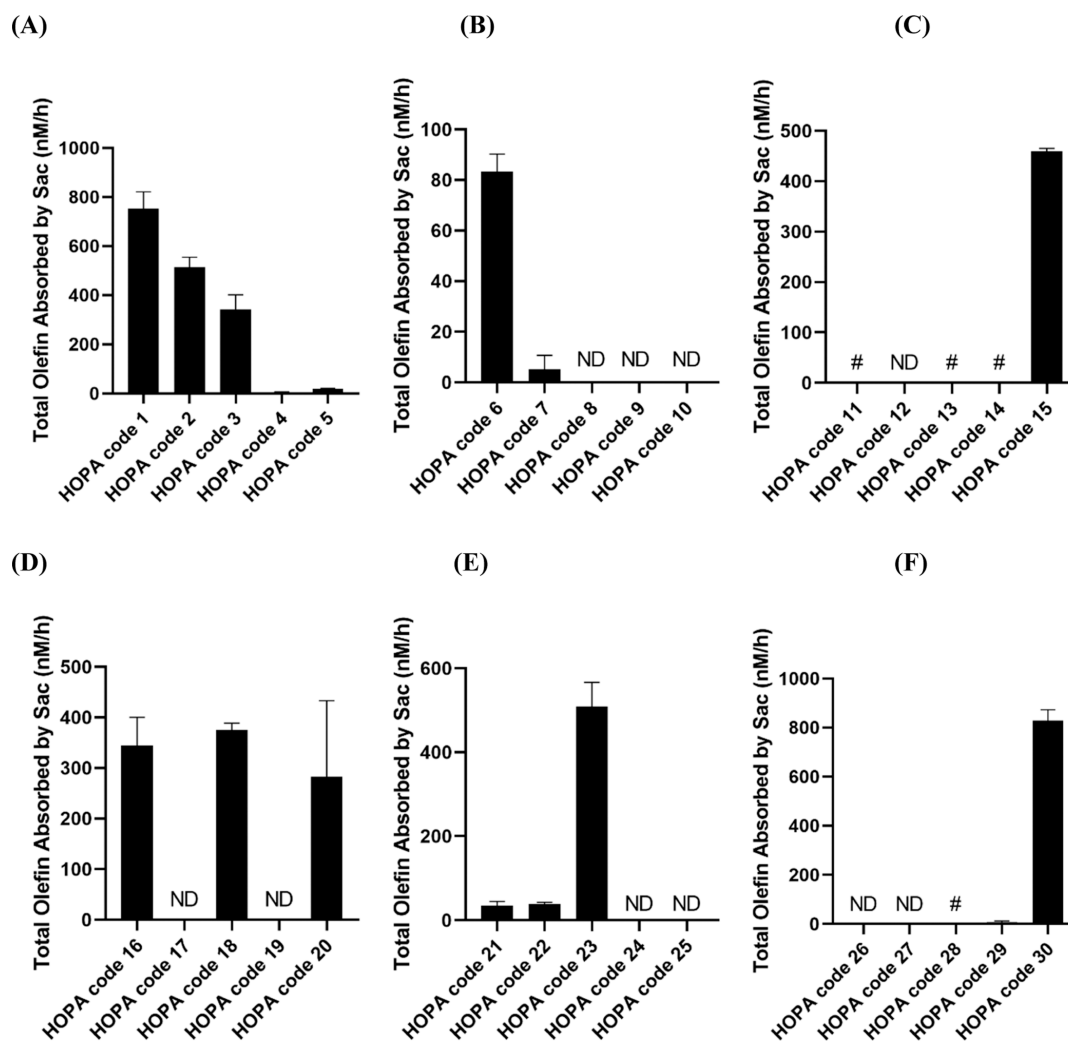
Figure 2. Total higher olefins absorbed by Sac nM/h. (A) Higher olefins with HOPA code from 1 to 5; (B) higher olefins with HOPA code from 6 to 10; (C) higher olefins with HOPA code from 11 to 15; (D) higher olefins with HOPA code from 16 to 20; (E) higher olefins with HOPA code from 21 to 25; and (F) higher olefins with HOPA code from 26 to 30.

estimation of lipophilicity of chemical compounds.[12] In addition, the in silico Caco-2 permeability models have been widely applied to assess absorption properties and the global obtained models showed accuracies between 78 and 82%.[13] Therefore, in the current study, both the lipophilicity (log P, 1-octanol/water partitioning coefficient) and the passive permeability across Caco-2 cell monolayers at pH 7.4 were calculated with ACD/Percepta v2018.2.1 software (ACD/Labs https://www.acdlabs.com/). The structure of C6, C8, and C20 with five configurations of the double bond for each carbon chain were analyzed, as well as 115 isomers.

2.7. Statistical Analysis. The GraphPad prism software version 8.0 was used for graphical representation and statistical analysis. Comparison between experimental groups was performed by analysis of variation (ANOVA), followed by Bonferroni's post-test. All values are expressed as mean ± SD and P values lower than 0.05 were considered statistically significant.

3. RESULTS

3.1. Intestinal Absorption Rates of Different Higher Olefins in the Everted Gut Sac Model. The absorption rate of each of the higher olefins was studied with 1 h incubation time. Results are shown in Figure 2 and Table 2. The absorption rate of iso-octene (C8, HOPA code 30) was the highest (16.2%, 829 nM/h), followed by that of 1-hexene (C6, HOPA code 1) (11.7%, 751 nM/h). Beside three substances that were insoluble

in the FeSSIF media, there were 10 substances that showed no measurable gut absorption after 1 h incubation: hexadec-1-ene—UVCB (C16, HOPA code 8), 1-octadecene—MC (C18, HOPA code 9), 1-octadecene—UVCB (C18, HOPA code 10), alkenes C20−24 α- (C22, HOPA code 12), hexadecane (C16, HOPA code 17), octadecene (C18, HOPA code 19), alkenes C15−18 (C16, HOPA code 24), alkenes C16−18 (C17, HOPA code 25), alkenes C19−23 (C21, HOPA code 26), and alkenes C20−24 (C23, HOPA code 27). In addition, 1-tetradecene-MC (C14, HOPA code 4) and 1-tetradecene-UVCB (C14, HOPA code 5) have an absorption rate less than 1% (4.1 and 17.7 nM/ h, respectively). Other higher olefins were absorbed between 1 and 10.9% (38.5 and 509 nM/h, respectively).

3.2. Relationship between Higher Olefin Absorption and Carbon Number. The C6, C8−C10 (C9 rich), and C10 molecules were readily absorbed into the intestinal sacs (Figure 2). Marked inter-compound differences were observed, with the amount of absorption generally decreasing with the increase in carbon number (Figure 3). Higher olefins with ≥14 carbons and over were either not absorbed or very poorly absorbed.

3.3. Prediction of Reactivity of Higher Olefins. To investigate the influence of the position and the substitution of the double bond on the reactivity, higher olefins with six and

Table 2. Percentage of Higher Olefins Absorbed by Sac per Hour[a]

HOPA code	name	the percentage (%) of total olefin absorbed by Sac per hour (mean ± SD)
1	1-hexene	11.7 ± 1.1
2	1-octene	10.0 ± 0.8
3	1-decene	8.1 ± 1.4
4	1-tetradecene-MC	0.1 ± 0.1
5	1-tetradecene-UVCB	0.6 ± 0.1
6	1-dodecene	2.3 ± 0.2
7	1-hexadecene-MC	0.2 ± 0.2
8	1-hexadecene-UVCB	ND
9	1-octadecene-MC	ND
10	1-octadecene-UVCB	ND
11	alkenes, C20−24 α-	insoluble
12	alkenes, C20−24 α-	ND
13	alkenes, C26−28 α-	insoluble
14	alkenes, C20 + α-	insoluble
15	octene	8.6 ± 0.1
16	decene	8.1 ± 1.3
17	hexadecene	ND
18	nonene	8.1 ± 0.3
19	octadecene	ND
20	alkenes, C10−14	7.9 ± 4.2
21	alkenes C11/C13/C14 (aka tridecene) (aka alkenes C13−14)	1.1 ± 0.3
22	alkenes C10/C11/C12/C13 (aka alkenes C11−12)	1.0 ± 0.1
23	alkenes, C8−10, C9-rich	10.9 ± 1.2
24	alkenes, C15−18	ND
25	alkenes, C16−18	ND
26	alkenes, C19−23 (aka hydrocarbons, C12−30, olefin-rich, ethylene polymn.by-product)	ND
27	alkenes, C20−24 (aka C20−C22 (even numbered, linear and branched) and C24 (branched) alkenes)	ND
28	alkenes, C24−28 (aka alkenes, C21−32 linear and branched)	insoluble
29	hexadecene	0.3 ± 0.2
30	iso-octene	16.2 ± 0.9

[a]ND: not detected.
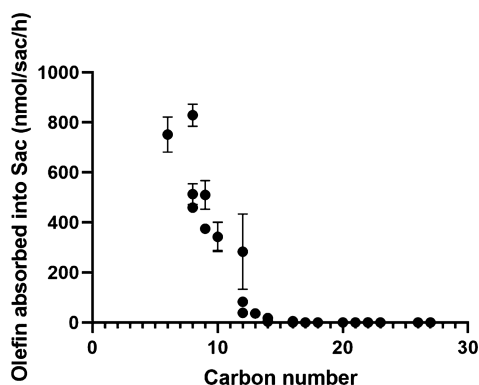
Figure 3. Relationship between higher olefin absorption and carbon number in vitro everted rat small intestinal sac model. Values are expressed as mean ± SD.

eight carbons were analyzed (shown in Figure 4a,b). Based on the HOMO−LUMO gap, four reactivity groups could be
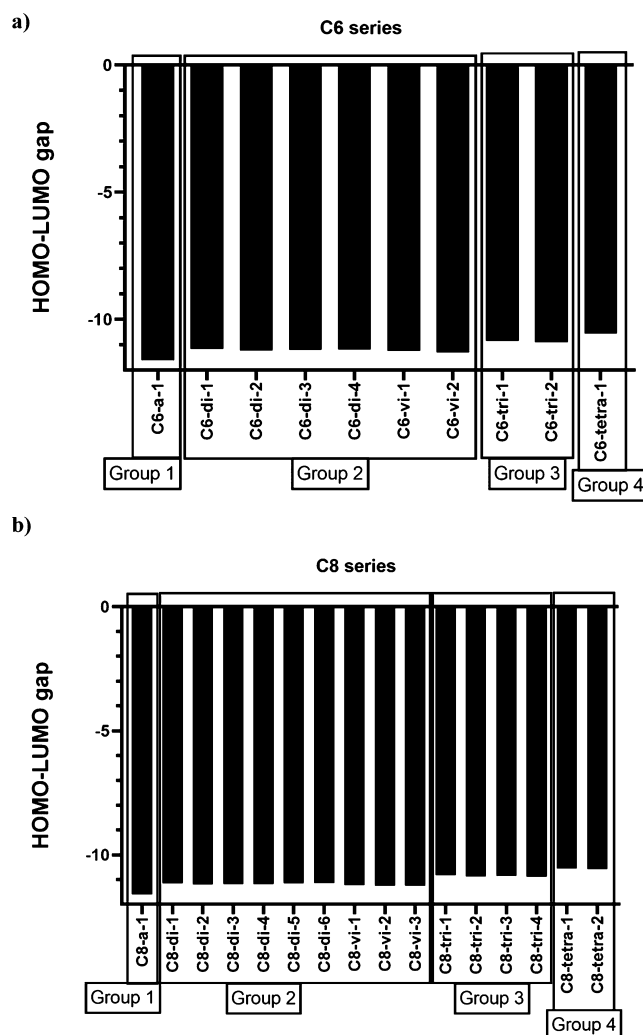
Figure 4. QM parameters (HOMO−LUMO gap) for (a) C6 series and (b) C8 series.

identified and characterized by a specific double bond type for both C6 and C8. Group 1 is the structure with a linear α double bond, which has the smallest HOMO−LUMO gap (highest reactivity), followed by group 2 which contains the structures with a linear internal and branched α (vinylidene) olefins. Group 3 comprises the branched internal—trisubstituted olefins. The branched internal—tetrasubstituted olefins group (group 4) showed the largest HOMO−LUMO gap (lowest reactivity).

To verify that the same group is also obtained when calculated for an increasing number of carbons, 20 isomers for C20 were randomly generated and analyzed (Figure 5a). As for C6 and C8 series, the same four reactivity groups were observed. In addition, when calculated for different numbers of carbon atoms (i.e., C6, C8, and C20), the same four reactivity groups were identified showing that isomers of the same reactivity group cluster together (Figure 5b). Moreover, group 2 can be subdivided into group 2A and 2B characterized by linear internal—disubstituted double bond olefins (2A) and branched α—vinylidene olefins (2B).

To cover the whole series of higher olefins, a data set of 115 isomers with the number of carbon atoms ranging from 6 to 28 and with five configurations of the double bond (α, disubstituted, trisubstituted, tetrasubstituted, and vinylidene) for each chain length were analyzed. As shown in Figure 6, the
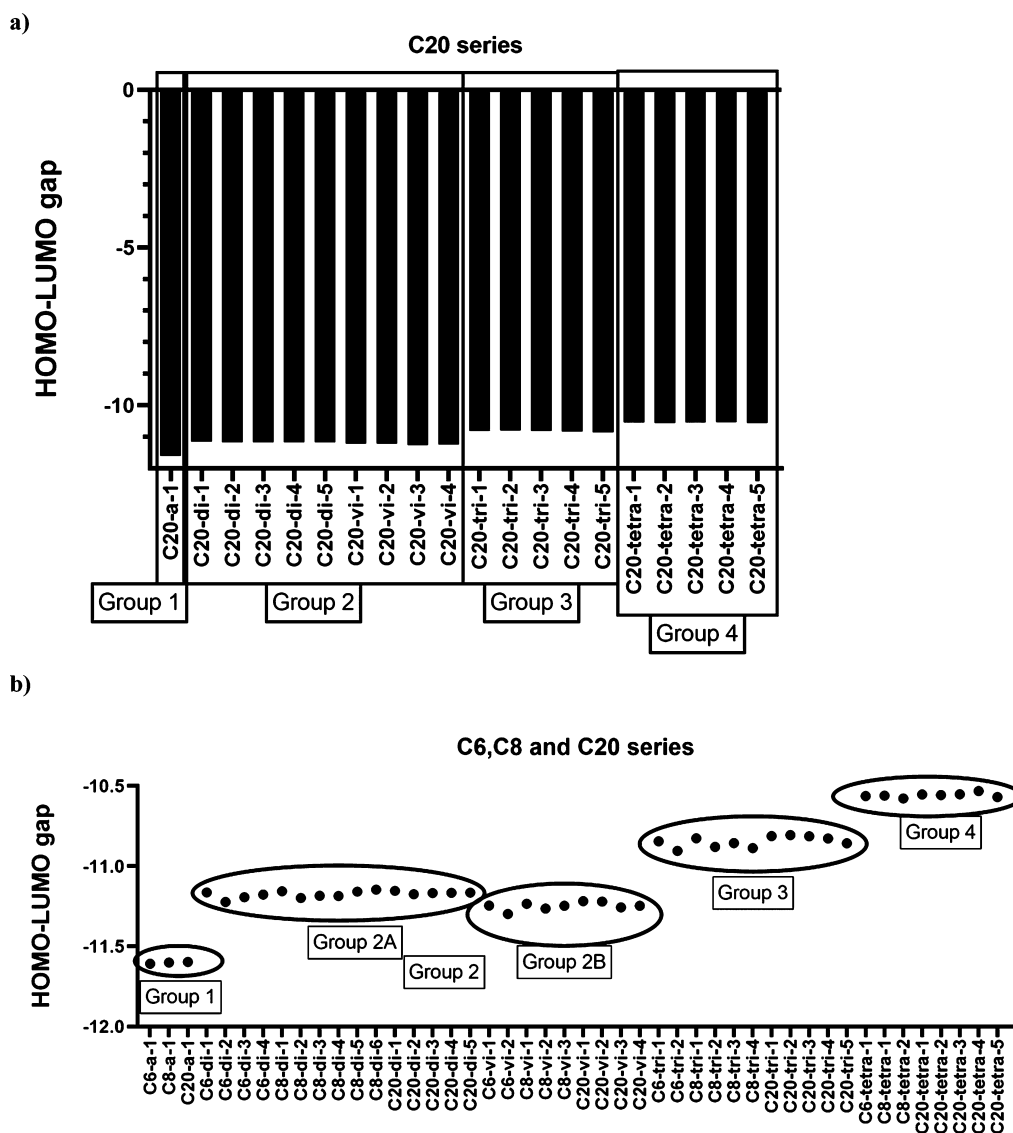
a)

b)

Figure 5. QM parameters (HOMO−LUMO gap) for (a) C20 series and (b) combination of C6, C8, and C20 series.

same four reactivity groups that were described above are found, well separated in the space of the QM descriptors.

3.4. Prediction of Lipophilicity and Permeability. To investigate the effect of the type of double bond as well as the carbon number on lipophilicity, isomers which cover for all five configurations of the double bond for C6, C8, and C20 were randomly generated. Figure 7a shows that the log P values were
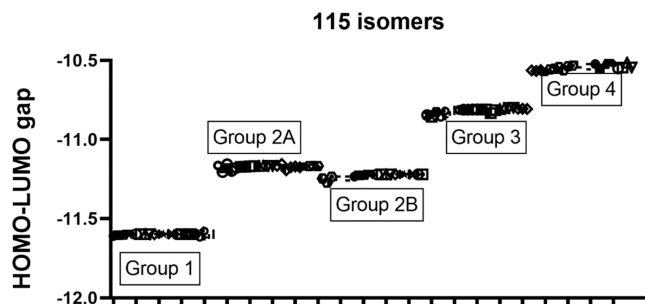
Figure 6. QM parameters (HOMO−LUMO gap) for 115 isomers, representing the whole series of olefins.

not influenced by the type of double bond among each carbon number. In addition, the log P values increased as the carbon number increased. Isomers with six carbons (C6) demonstrated similar log P values as isomers with eight carbons (C8), while isomers with 20 carbons (C20) showed the highest log P values.

Caco-II values of C6, C8, and C20 were calculated and represent the permeability (Figure 7b). In contrast to lipophilicity, the permeability decreased with the increase in carbon number. Overall, C6 and C8 showed comparable permeability, and C20 demonstrated approximately 7600-fold lower permeability than C6 and C8. In addition, no difference was observed for each carbon chain among the different types of double bond.

To demonstrate whether similar patterns for both lipophilicity and permeability were also observed for the whole series of higher olefins, the 115 isomers (listed in Table S3 of the Supporting Information) which were generated previously were analyzed (Figure 8). In Figure 8a, log P values showed a clear increasing trend as the carbon number increased, while no difference was observed among each type of double bond with the same carbon number. Similarly, the permeability decreased when the carbon number increased, and again no influence by
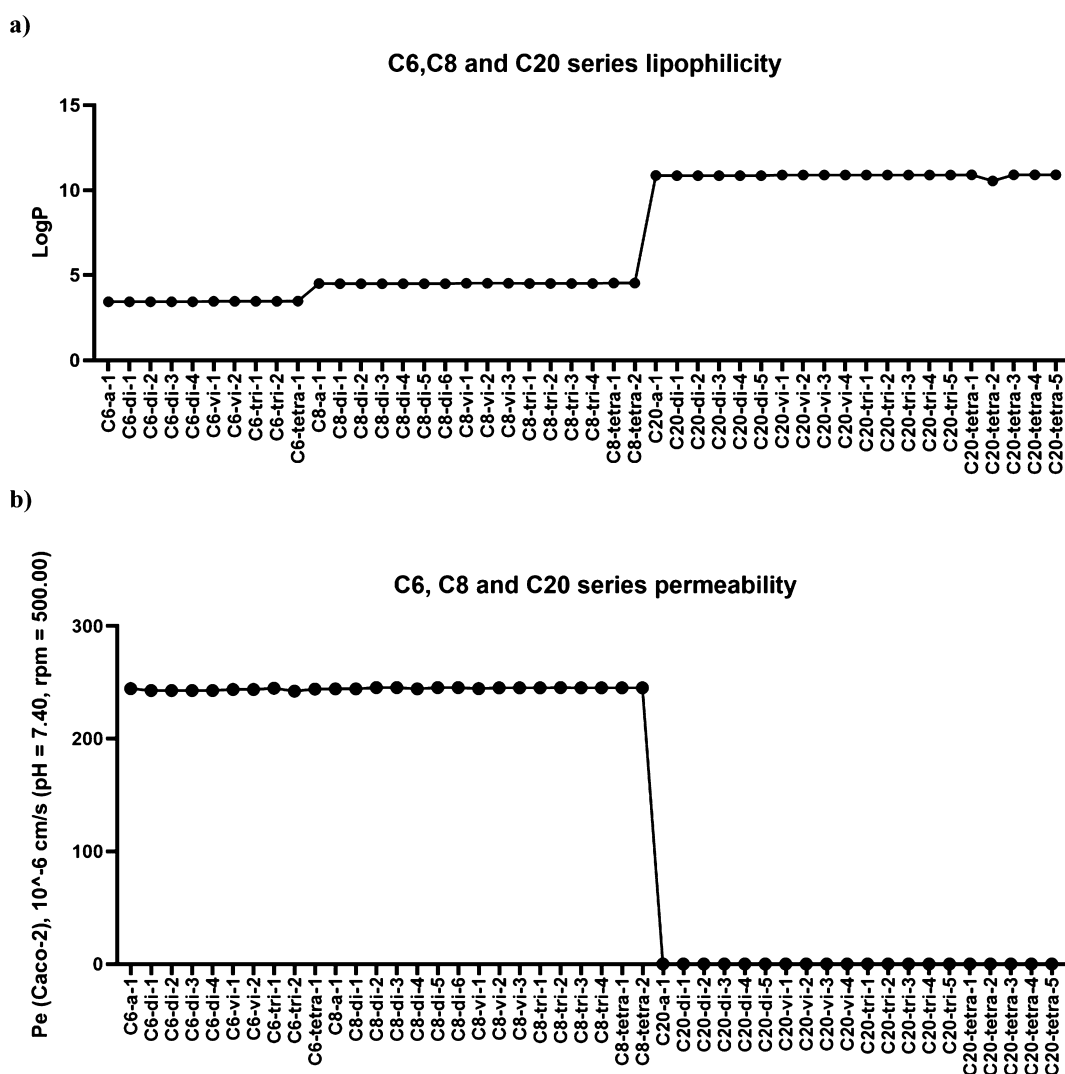
a)

b)

Figure 7. a) Log *P* value of C6, C8, and C20 series; (b) Caco-II value of C6, C8, and C20 series.

the number of carbon atoms was observed. In addition, the permeability decreased, while lipophilicity increased (Figure 8c).

4. DISCUSSION

Despite the frequent use of higher olefins, limited information is available on their bioavailability. The isolated everted rat intestine has been used to study the absorption of a variety of materials and is recognized as an excellent model for the study of the passage of substances through the gut wall.[14] Therefore, in the current study, the absorption rate of a group of higher olefins (Table 1) was determined using the everted gut sac model. It was shown that the amount of absorption generally decreased with the increase in carbon number, and higher olefins with ≥C14 carbons were either not absorbed or very poorly absorbed. In addition, an in silico approach was applied in the current study to predict the reactivity and intestinal permeability of a series of higher olefins comprising a total of 115 isomers which included olefins with the number of carbon atoms ranging from 6 to 28 and with all five configurations of the double bond (α, di-substituted, tri-substituted, tetra-substituted, and vinyl). The permeability simulation results corroborated the findings from the everted gut sac model experiments.

The mechanism of intestinal absorption involves passive diffusion and/or active transport.[15] Passive diffusion comprises two pathways: the paracellular pathway, in which the substance diffuses through the aqueous pores at the tight junctions between the intestinal enterocytes and the transcellular (lipophilic) pathway, which requires the substance to diffuse across the lipid cell membrane of the enterocyte. The active transport pathway is mediated by transporters and is divided into active influx and efflux of the substance. Higher olefins are expected to be absorbed through the transcellular pathway as all the higher olefins have a log *P* value greater than 0. Meanwhile, the log *P* values (molecular descriptor for lipophilicity) were calculated for 115 higher olefins isomers and it was shown that the lipophilicity increases with the increase in carbon number regardless of the chemical structure of the isomers. It is generally assumed that more lipophilic compounds will diffuse faster across the cellular membranes of the intestinal epithelium, which constitutes the main barrier for oral absorption. This implies that with an increase in the molecular weight of higher olefins, the absorption rate will also increase. However, we showed a clear trend of decreasing absorption rate of higher olefins with the increase in lipophilicity.

To further explain the observed trend, the data were compared to other substances with similar carbon chain lengths
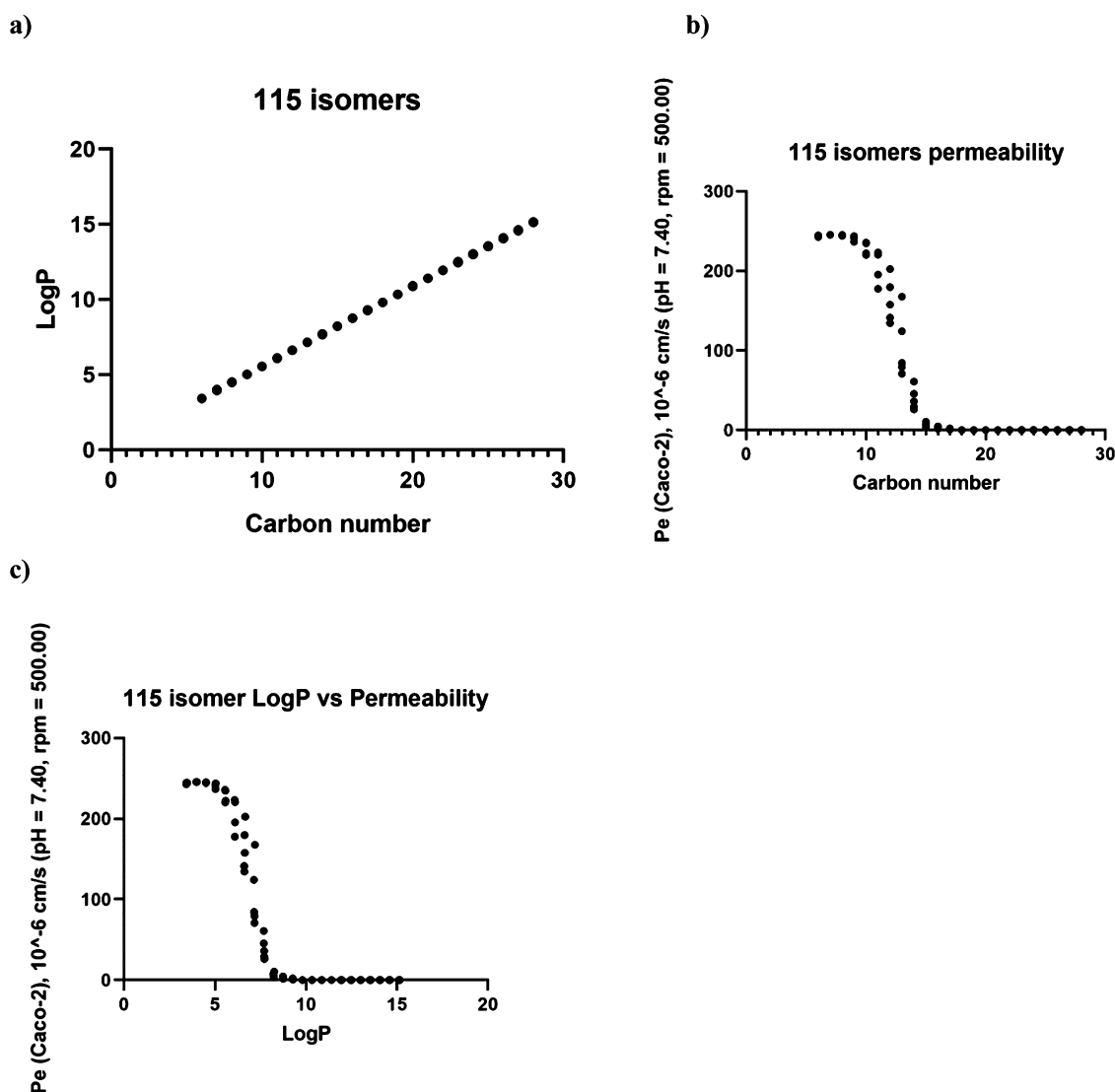
a)

b)

c)

Figure 8. a) Scatter plot of log P values vs carbon number for the data set of 115 isomers; (b) Caco-II value vs carbon number for the data set of 115 isomers; and (c) log P values vs Caco-II values for the data set of 115 isomers.

as the higher olefins such as dietary-derived fatty acids. The apparently poor absorption of higher olefins with chain lengths greater than C14 is in apparent conflict with fatty acids, derived from the lipase-mediated hydrolysis of dietary triglycerides in the small intestine, which are readily absorbed.[16] This difference between fatty acids and olefins of the same carbon chain length is due to the ionizable carboxylic acid function of the fatty acids. At the pH found in the small intestine, depending on individual pKa values, considerable amounts of the fatty acids exist as carboxylate anions. Short- and medium-chain fatty acids (<C14) are absorbed directly into the blood via intestinal capillaries and travel through the portal vein just as other absorbed nutrients do.[17] However, long-chain fatty acids are not directly absorbed into the intestinal capillaries. Instead, they are absorbed into the fatty walls of the intestinal villi and reassembled again into triglycerides. For this, they obviously require the carboxylic acid functional group. In addition, a considerable fraction of the fatty acids also enter the enterocyte via a specific fatty acid transporter protein in the membrane. In contrast to fatty acids, a similar trend with highly lipophilic substances showing low absorption is also often observed in drug research. A series of drugs were examined for their potential

to enter intestinal epithelial cells, and it was found that a lipophilicity of around 3 corresponded to an optimal trans-epithelial passage of drugs but that a higher lipophilicity would result in lower intestinal epithelial permeability.[18] Because all higher olefins have predicted log P value greater than 3 (3.43 is the lowest log P value calculated), this would indicate that the higher olefins fall in the range of lipophilicity with a negative correlation with intestinal permeability.

In the current study, the reactivity of higher olefins was analyzed because it is one of the key parameters with regard to oral bioavailability and presented by QM. QM is a fundamental theory in physics which describes nature at the smallest scales of energy levels of atoms and subatomic particles.[19] The theory applied in the current analysis is the molecular orbital (MO) theory which is a method for describing the electronic structure of molecules using QM.[20] Electrons are not assigned to individual bonds between atoms, but are treated as moving under the influence of the nuclei in the whole molecule. The spatial and energetic properties of electrons are described by QM as MOs surround two or more atoms in a molecule and contain valence electrons between atoms. The energies of HOMO (highest occupied MO) and LUMO (lowest

Figure 9. Hazard matrix of higher olefins based on carbon number and type of double bond. Red: high hazard; orange: medium hazard; and green: low hazard.

unoccupied MO) are related to the reactivity of the molecule:[21] molecules with electrons at accessible (near-zero) HOMO levels tend to be good nucleophiles because it does not cost much to donate these electrons toward making a new bond. Similarly, molecules with low LUMO energies tend to be good electrophiles because it does not cost much to place an electron into such an orbital. Therefore, the larger HOMO−LUMO gap refers to higher kinetic stability and lower chemical reactivity of the molecule. The HOMO−LUMO gap and the HOMO energy were considered in this analysis to assess both the general reactivity of the molecule and the nucleophilic character of the double bond. The nucleophilic character of the double bond is correlated specifically to the epoxide formation: the more nucleophilic is the double bond, the easier is the formation of the epoxide.[22] The results of the simulations show that all the tested higher olefins can be split into four reactivity groups which were separated by the position of the double bond rather than carbon number. Furthermore, olefins with a linear α double bond are the most reactive, followed by olefins with a linear internal and branched internal (vinylidene) double bond, and then branched internal—trisubstituted double bond with branched internal—tetrasubstituted double bond finally showing the lowest reactivity compared with the other olefins. Olefins are oxidized by hepatic microsomal enzymes to glycols (diols) via an epoxide intermediate, followed by hydrolysis of the oxirane ring by epoxide hydrolase. These current results are further supported by in vitro studies which demonstrated that the metabolism of olefins to glycolyse faster for α-olefins than internal- and branched chain olefins.[23,24] This phenomenon is explained by steric hindrance assuming that the metabolic process is readily accessible for linear α double bonds but relatively inaccessible for other types of double bonds.[24] In addition, another in vitro study, using hepatic microsomal fractions from phenobarbital induced rats, demonstrated the loss of cytochrome P-450 due to alkylation of the haem function, leading to the loss of the monooxygenase activity, occurring to a greater extent with linear and branched α olefins than with internal olefins (with or without branching) for which no or minimal loss of cytochrome P-450 activity was detected.[25] The authors suggested that α olefins are biologically more reactive than internal and/or branched olefins.

Based on the information mentioned above, a hazard matrix for higher olefins based on two parameters (i.e., carbon number and double bond type) is proposed (Figure 9). Higher olefins with short carbon chain lengths and a linear α double bond are the most toxic, and this toxicity decreases with the increase in chain lengths as well as the type of double bond in the following order: linear α > branched α—vinylidene > linear internal—disubstituted > branched internal—trisubstituted > branched internal—tetrasubstituted. This matrix can assist not only in the selection of the source compounds for read-across and/or higher

tier testing by identifying a worst case scenario but also in the interpretation of differences observed in studies with other higher olefins.

5. CONCLUSIONS

The absorption rate was determined of a series of higher olefins (with carbon chain lengths ranging from 6 to 28 and with five configurations of the double bond) in the everted rat small intestine gut sac model showing that intestinal absorption decreases dramatically with the increase in carbon chain length. In addition, in silico approaches provided further information on how lipophilicity varies across the group of higher olefins and how this variation impacts the Caco-2 permeability, which correlates with the oral absorption. A data matrix was developed that aided in the read-across justification and also supported the read-across hypothesis among the higher olefins category and helped to explain the differences in toxicity observed.

The author(s) declared the following potential conflicts of interest with respect to the research, authorship, and/or publication of this article: the authors of this article are either employed by companies that manufacture petroleum products or consultants.

◼ ASSOCIATED CONTENT

Ⓢ Supporting Information

The Supporting Information is available free of charge at https://pubs.acs.org/doi/10.1021/acs.chemrestox.2c00089.

SMILES and structures of series C6, C8, and C20 and SMILES of the 115 isomers (PDF)

◼ AUTHOR INFORMATION

Corresponding Authors

Quan Shi − *Shell Global Solutions International B.V., The Hague 2596HR, The Netherlands;* ⓞ orcid.org/0000-0001-8491-9548; Email: quan.shi@shell.com

Jason Manton − *Penman Consulting Ltd., Oxon OX12 9FF, U.K.;* Email: jason.manton@penmanconsulting.com

Authors

Juan-Carlos Carrillo − *Shell Global Solutions International B.V., The Hague 2596HR, The Netherlands*

Michael G. Penman − *Penman Consulting Ltd., Oxon OX12 9FF, U.K.*

Elena Fioravanzo − *ToxNavigation Ltd., East Molesey KT9 8HW, U.K.*

Robert H. Powrie − *CXR Biosciences Ltd., Dundee DD1 5JJ, U.K.*

Clifford R. Elcombe − *CXR Biosciences Ltd., Dundee DD1 5JJ, U.K.*

Tilly Borsboom-Patel − *Penman Consulting Ltd., Oxon OX12 9FF, U.K.*

Yuan Tian − *University College London, London EC1V 9EL, U.K.*

Hua Shen − *Shell Oil Company, Houston, Texas 77079, United States*

Peter J. Boogaard − *Division of Toxicology, Wageningen University and Research, 6708 WE Wageningen, The Netherlands*

Complete contact information is available at:
https://pubs.acs.org/10.1021/acs.chemrestox.2c00089

■ **REFERENCES**

(1) Dean, J. A. *Lange's Handbook of Chemistry*; McGraw-Hill, Inc.: New York; London, 1999.

(2) Froment, G. F. Thermal cracking for olefins production. Fundamentals and their application to industrial problems. *Chem. Eng. Sci.* **1981**, *36*, 1271−1282.

(3) Council, A. C. *A Comparison of the Environmental Performance of Olefin and Paraffin Synthetic Base Fluids (SBF)*, 2006.

(4) Schroeder, K.; Bremm, K. D.; Alépée, N.; Bessems, J. G. M.; Blaauboer, B.; Boehn, S. N.; Burek, C.; Coecke, S.; Gombau, L.; Hewitt, N. J.; et al. Report from the EPAA workshop: In vitro ADME in safety testing used by EPAA industry sectors. *Toxicol. in Vitro* **2011**, *25*, 589−604.

(5) Nigsch, F.; Klaffke, W.; Miret, S. In vitro models for processes involved in intestinal absorption. *Expert Opin. Drug Metab. Toxicol.* **2007**, *3*, 545−556.

(6) (a) Alam, M. A.; Al-Jenoobi, F. I.; Al-Mohizea, A. M. Everted gut sac model as a tool in pharmaceutical research: limitations and applications. *J. Pharm. Pharmacol.* **2012**, *64*, 326−336. (b) Barthe, L.; Woodley, J.; Houin, G. Gastrointestinal absorption of drugs: methods and studies. *Fundam. Clin. Pharmacol.* **1999**, *13*, 154−168.

(7) Artursson, P.; Karlsson, J. Correlation between oral drug absorption in humans and apparent drug permeability coefficients in human intestinal epithelial (Caco-2) cells. *Biochem. Biophys. Res. Commun.* **1991**, *175*, 880−885.

(8) Wilson, T. H.; Wiseman, G. Metabolic activity of the small intestine of the rat and golden hamster (Mesocricetus auratus). *J. Physiol.* **1954**, *123*, 126−130.

(9) Iannaccone, P. M.; Jacob, H. J. Rats! *Dis. Models Mech.* **2009**, *2*, 206−210.

(10) Hryn, V. H.; Kostylenko, Y. P.; Yushchenko, Y. P.; Lavrenko, A. V.; Ryabushko, O. B. General comparative anatomy of human and white rat digestive systems: a bibliographic analysis. *Wiad. Lek.* **2018**, *71*, 1599−1602.

(11) Czyrski, A. Determination of the Lipophilicity of Ibuprofen, Naproxen, Ketoprofen, and Flurbiprofen with Thin-Layer Chromatography. *J. Chem.* **2019**, *2019*, 1.

(12) Kujawski, J.; Popielarska, H.; Myka, A.; Drabińska, B.; Bernard, M. The log P Parameter as a Molecular Descriptor in the Computer-aided Drug Design—an Overview. *CMST* **2012**, *18*, 81−88.

(13) (a) Pham-The, H.; Cabrera-Pérez, M. Á.; Nam, N.-H.; Castillo-Garit, J. A.; Rasulev, B.; Le-Thi-Thu, H.; Casañola-Martin, G. M. In Silico Assessment of ADME Properties: Advances in Caco-2 Cell Monolayer Permeability Modeling. *Curr. Top. Med. Chem.* **2019**, *18*, 2209−2229. (b) Pham The, H.; González-Alvarez, I.; Bermejo, M.; Mangas Sanjuan, V.; Centelles, I.; Garrigues, T. M.; Cabrera-Pérez, M. Á. In Silico Prediction of Caco-2 Cell Permeability by a Classification QSAR Approach. *Mol. Inf.* **2011**, *30*, 376−385.

(14) Nolan, J. P.; Hare, D. K.; McDevitt, J. J.; Vilayat Ali, M. In Vitro Studies of Intestinal Endotoxin Absorption. *Gastroenterology* **1977**, *72*, 434−439.

(15) (a) El-Kattan, A.; Varm, M. Oral absorption, intestinal metabolism and human oral bioavailability. *Top. Drug Metab.* **2012**, *10*, 31087. (b) Liu, Z.; Wang, S.; Hu, M. Chapter 11—Oral Absorption Basics: Pathways, Physico-chemical and Biological Factors Affecting Absorption. In *Developing Solid Oral Dosage Forms*; Qiu, Y., Chen, Y., Zhang, G. G. Z., Liu, L., Porter, W. R., Eds.; Academic Press, 2009; pp 263−288.

(16) Clément, J. [Digestion and absorption of dietary triglycerides]. *J. Physiol.* **1976**, *72*, 137−170.

(17) Sigalet, D. L.; Winkelaar, G. B.; Smith, L. J. Determination of the route of medium-chain and long-chain fatty acid absorption by direct measurement in the rat. *JPEN, J. Parenter. Enteral Nutr.* **1997**, *21*, 275−278.

(18) Wils, P.; Warnery, A.; Phung-Ba, V.; Legrain, S.; Scherman, D. High lipophilicity decreases drug transport across intestinal epithelial cells. *J. Pharmacol. Exp. Ther.* **1994**, *269*, 654−658.

(19) Feynman, R. P.; Leighton, R. B.; Sands, M.; Hafner, E. M. The feynman lectures on physics; vol. i. *Am. J. Phys.* **1965**, *33*, 750−752.

(20) Daintith, J. *The Facts on File Dictionary of Inorganic Chemistry*; Infobase Publishing, 2004.

(21) Griffith, J. S.; Orgel, L. E. Ligand-field theory. *Q. Rev., Chem. Soc.* **1957**, *11*, 381−393.

(22) (a) Apeloig, Y.; Karni, M.; Rappoport, Z. Nucleophilic attacks on carbon-carbon double bonds. Part 29. Role of hyperconjugation in determining the stereochemistry of nucleophilic epoxidation and cyclopropanation of electrophilic olefins. *J. Am. Chem. Soc.* **1983**, *105*, 2784−2793. (b) Swallow, W. H. Reactions of epoxides with neighbouring nucleophiles. Ph.D. Thesis, University of Canterbury, 1972.

(23) Leibman, K. C.; Ortiz, E. Epoxide intermediates in microsomal oxidation of olefins to glycols. *J. Pharmacol. Exp. Ther.* **1970**, *173*, 242−246.

(24) Maynert, E. W.; Foreman, R. L.; Watabe, T. Epoxides as obligatory intermediates in the metabolism of olefins to glycols. *J. Biol. Chem.* **1970**, *245*, 5234−5238.

(25) Ortiz de Montellano, P. R.; Mico, B. A. Destruction of cytochrome P-450 by ethylene and other olefins. *Mol. Pharmacol.* **1980**, *18*, 128−135.